Pantopteron: A New Fully Decoupled 3DOF Translational Parallel Robot for Pick-and-Place Applications

S. Briot
e-mail: sebastien.briot.1@ens.etsmtl.ca

I. A. Bonev
e-mail: ilian.bonev@etsmtl.ca

Department of Automated Manufacturing Engineering,
École de Technologie Supérieure (ÉTS),
Montreal, QC, H3C1K3, Canada

In this paper, a novel 3DOF fully decoupled translational parallel robot, called the Pantopteron, is presented. This manipulator is similar to the Tripteron Cartesian parallel manipulator, but due to the use of three pantograph linkages, an amplification of the actuator displacements is achieved. Therefore, equipped with the same actuators, the mobile platform of the Pantopteron moves many times faster than that of the Tripteron. This amplification is defined by the magnification factor of the pantograph linkages. The kinematics, workspace, and constraint singularities of the proposed parallel robot are studied in detail. Design considerations are also discussed, and a possible prototype is illustrated. [DOI: 10.1115/1.3046125]

Keywords: translational parallel robot, isotropy, input-output decoupling, constrained singularity, workspace, design

1 Introduction

Less than a decade ago, any known parallel robot with three or more degrees of freedom (DOFs) was inevitably associated with nonlinear highly coupled kinematics, singularities, and a complex-shaped workspace. In May 2001, a revolutionary simple 3DOF translational parallel robot, with *fully decoupled* input-output equations, was disclosed by Gosselin and Kong [1] in a Canadian provisional patent application. Its simplest design, illustrated in Fig. 1(*a*), is basically a *Cartesian robot* and is therefore *isotropic* (its Jacobian matrix is diagonal and constant). After careful investigation, Kong and Gosselin [3,4], helped by the second author of this paper, drafted a patent application that covers all possible design variations. Each of these variations, named Tripteron, is now patent protected in many countries, including the USA.

Later in 2002, Carricato and Parenti-Castelli [2] and Kong and Gosselin [3,4] proposed separately a large family of decoupled 3DOF translational parallel mechanisms, all covered by the above-mentioned patent. At the same time, Kim and Tsai [5] presented independently the simplest member of this family (the one shown in Fig. 1(*a*)).

Who among these three groups of researchers was the first to invent the 3DOF isotropic parallel robot is not the subject of this paper. In fact, a synthesis of possible legs for the mechanism in Fig. 1(*a*) was presented in Ref. [6] as early as in 1991. What is obvious is that the year 2002 marked the beginning of worldwide research activities on isotropic parallel mechanisms.

The most prolific author on this subject, Gogu, wrote dozens of papers and even a 700-page manuscript [7] proposing isotropic architectures for nearly all combinations of translational and rotational degrees of freedom. Among these papers, Ref. [8] proposes other variations of the Tripteron family. Specific members from the Tripteron family were studied in detail in many works (e.g., Refs. [9–13]).

The basic Tripteron parallel robot consists of three identical legs. Each leg has a base-mounted actuator, allowing translation along a fixed direction, and a planar chain. To make the mechanism isotropic, the planes of motion of the three planar chains should be orthogonal. Some of the joints of the planar chains may actually be replaced with higher-degree pairs, such as a universal joint, but this has no effect on the kinematics of the mechanism.

In the basic Tripteron, the displacement of the mobile platform along a given Cartesian axis is directly proportional to the displacement of each linear actuator. When the plane of the planar chain in a leg is normal to the direction of the corresponding linear actuator (as in the mechanism of Fig. 1(*a*)), there is a one-to-one relationship, and the Jacobian matrix is the identity matrix. Otherwise, larger displacements are needed from the actuators to produce smaller motions at the mobile platform (as in the mechanism of Fig. 1(*b*)).

However, as we recently witnessed with the commercialization of the Quattro robot by Adept Technology, Livermore, CA [14], the only way to compete with the hugely successful Delta pick-and-place robot [15] is to offer an even faster design. Hence, it would have been great if we could build a Tripteron with an amplification factor. Not only would this robot be isotropic, but it might also move several times faster than its linear actuators.

This paper is the first to provide such a solution through the use of pantographs. Of course, the proposed design is more complicated than the simplest Tripteron of Fig. 1(*a*), but this seems to be a reasonable price to pay. Indeed, the proposed design is the result of a large study on the synthesis of parallel manipulators using pantographs [16]. One such manipulator was already successfully built and proves the viability of using pantographs [17].

This paper is organized as follows. Next, the kinematics of the proposed design, named the Pantopteron, is presented. The structure is described, and its movements are analyzed, as well as their singularities. Then, its workspace is studied, and various design considerations are given. Finally, conclusions are drawn.

2 Kinematic Analysis

2.1 Description of the Architecture. The architecture of the Pantopteron is schematized in Fig. 2. It is composed of three identical legs, which correspond to pantograph linkages (Fig. 3).

The pantograph is a mechanical system with two input points, A_i and B_i, and one output point C_i (in the remainder of this paper, $i=1,2,3$). These input points linearly control the displacement of output point C_i. A kinematic analysis shows that a linear actuator

Contributed by the Mechanisms and Robotics Committee of ASME for publication in the JOURNAL OF MECHANISMS AND ROBOTICS. Manuscript received June 16, 2008; final manuscript received September 10, 2008; published online January 6, 2009. Review conducted by Jean-Pierre Merlet.

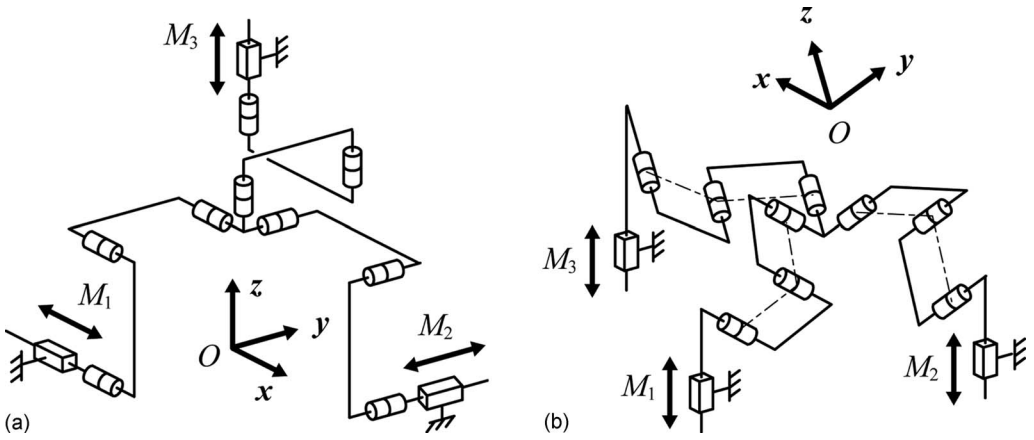

Fig. 1 Two versions of the Tripteron. (*a*) The directions of the actuators are orthogonal and (*b*) the directions of the actuators are parallel.

connected with input point B_i controls the vertical displacement of the output point C_i, and another linear actuator with an axis parallel to $\mathbf{a}_{1i}$ controls the displacements along the same axis. Note that these motions are completely decoupled; i.e., they can be carried out independently. The input/output relationships for displacements are linear and are determined by the magnification factor k of the pantograph ($k=A_iC_i/A_iB_i$). These properties of the pantograph mechanism are used in the Pantopteron.

For the Pantopteron, the actuators are located at the linear pairs ($1i$) (Fig. 3). These three pairs are connected to the base so that their axes are orthogonal. All other joints are passive. Each pantograph linkage is attached to the platform at point C_i via a Cardan joint, the axes of each joint ($12i$) being orthogonal. They are also connected to actuator ($1i$) via a revolute joint, which allows the leg to have five DOFs, three translations, and two rotations about the axes of the Cardan joint located at C_i. Such an architecture allows three fully decoupled translational DOFs. This will now be proved.

2.2 Mobility Analysis. Let $\boldsymbol{x}$, $\boldsymbol{y}$, and $\boldsymbol{z}$ be the axes of the base frame (Fig. 2). Without loss of generality, let us consider the displacements of the platform when legs 2 and 3 are disconnected, as well as the actuator M_1 located at pair (1,1). A simple analysis could show that the platform has five passive DOFs, three translations, and two rotations (one about the axis of pair (11,1) and another about the axis of pair (12,1)). Therefore, leg 1 applies one wrench on the platform that constrains its displacements. This wrench is the reciprocal screw to the twists of each passive displacement of the platform.

We denote as $\mathbf{e}_j$ ($j=1-5$) the unit screw corresponding to the passive displacement of the platform. The expression of these screws, expressed in the base frame at point C_1, can be written as follows:

- for the translations along $\boldsymbol{x}$, $\boldsymbol{y}$, and $\boldsymbol{z}$, $\mathbf{e}_{11}=[0\ 0\ 0\ 1\ 0\ 0]^T$, $\mathbf{e}_{21}=[0\ 0\ 0\ 0\ 1\ 0]^T$, and $\mathbf{e}_{31}=[0\ 0\ 0\ 0\ 0\ 1]^T$
- for the rotations about the axes of pairs (12,1) and (11,1), $\mathbf{e}_{41}=[\cos\gamma_1\ \cos\theta_1 \sin\gamma_1\ \sin\theta_1 \sin\gamma_1\ 0\ 0\ 0]^T$ and $\mathbf{e}_{51}=[0\ -\sin\theta_1\ \cos\theta_1\ 0\ 0\ 0]^T$, where θ_1 is the angle between $\mathbf{a_{11}}$ and $\boldsymbol{y}$ axes, and γ_1 represents the rotation between vector $\mathbf{a_{31}}$ and the axis of pair (12,1)

The Plücker coordinates of the unit screws can be described in matrix $\mathbf{E_1}$ as

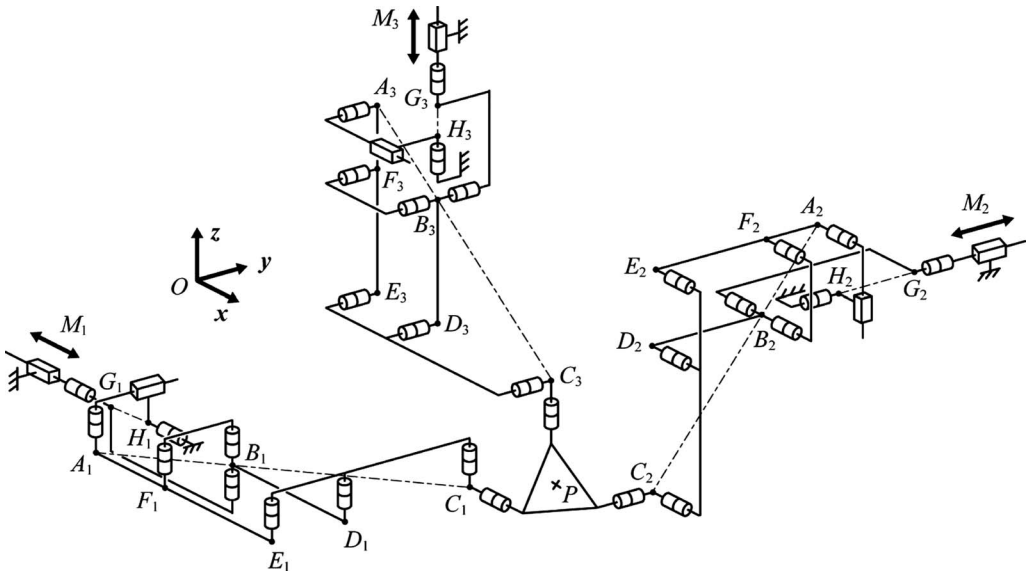

Fig. 2 Schematics of the Pantopteron

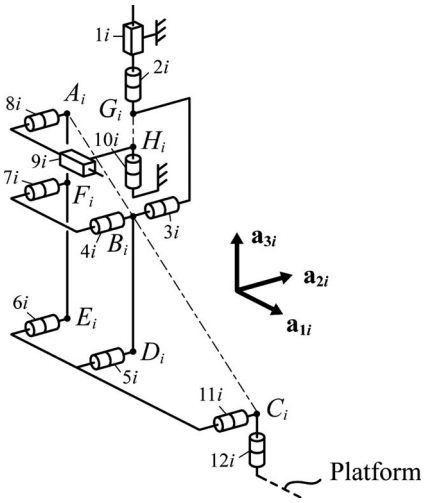

Fig. 3 Schematics of a leg of the Pantopteron

$$\mathbf{E_1} = \begin{bmatrix} \mathbf{e}_{11}^T \\ \mathbf{e}_{21}^T \\ \mathbf{e}_{31}^T \\ \mathbf{e}_{41}^T \\ \mathbf{e}_{51}^T \end{bmatrix} = \begin{bmatrix} 0 & 0 & 0 & 1 & 0 & 0 \\ 0 & 0 & 0 & 0 & 1 & 0 \\ 0 & 0 & 0 & 0 & 0 & 1 \\ \cos\gamma_1 & \cos\theta_1 \sin\gamma_1 & \sin\theta_1 \sin\gamma_1 & 0 & 0 & 0 \\ 0 & -\sin\theta_1 & \cos\theta_1 & 0 & 0 & 0 \end{bmatrix} \tag{1}$$

The wrench $\mathbf{r_{11}}$, transmitted to the platform by the leg, is orthogonal to the twists composing the lines of matrix $\mathbf{E_1}$:

$$\mathbf{r_{11}} = [r_{11}^x \quad r_{11}^y \quad r_{11}^z \quad 0 \quad 0 \quad 0]^T \tag{2}$$

with

$$r_{11}^x = -\sin\gamma_1 \tag{3a}$$

$$r_{11}^y = \cos\theta_1 \cos\gamma_1 \tag{3b}$$

$$r_{11}^z = \sin\theta_1 \cos\gamma_1 \tag{3c}$$

Thus, $\mathbf{r_{11}}$ is a wrench of zero pitch (a pure moment).

Similarly, it is possible to find that the wrenches $\mathbf{r_{1}}_i$ transmitted to the platform by the legs when all actuators are disconnected are all pure moments. Let $\mathbf{Q}$ be the matrix composed of these wrenches applied on the platform by the legs. The expression of $\mathbf{Q}$ in the base frame, and expressed at point O, is

$$\mathbf{Q} = \begin{bmatrix} \mathbf{r}_{11}^T \\ \mathbf{r}_{12}^T \\ \mathbf{r}_{13}^T \end{bmatrix} = \begin{bmatrix} r_{11}^x & r_{11}^y & r_{11}^z & 0 & 0 & 0 \\ r_{12}^x & r_{12}^y & r_{12}^z & 0 & 0 & 0 \\ r_{13}^x & r_{13}^y & r_{13}^z & 0 & 0 & 0 \end{bmatrix} \tag{4}$$

The twists defining the passive displacements of the platform are orthogonal to this matrix of rank equal to 3. In the general case, there are three independent passive displacements, which are the three translations about $\boldsymbol{x}$, $\boldsymbol{y}$, and $\boldsymbol{z}$ axes. Thus, the platform is constrained by the legs to have only translational displacements.

Note that in some cases where the three wrenches are linearly dependent, the platform gains one additional DOF. This case will be treated later in the section about singularities.

Let us now consider that the actuator M_1 located at pair (1,1) is fixed. So, due to the decoupling properties of the pantograph linkages, the position about the $\boldsymbol{x}$ axis of point C_1 is fixed. Thus, the platform has now two passive translational DOFs, which are orthogonal to the $\boldsymbol{x}$ axis. Therefore, a supplementary constraint is applied on the platform, which restrains its displacement.

Using an approach similar to the previous one, the second wrench applied by the leg on the platform, expressed at point C_1, is $\mathbf{r_{21}}=[0\ 0\ 0\ 1\ 0\ 0]^T$. By a similar analysis, is can be seen that when the three legs are connected to the platform and the actuators M_i are fixed, six wrenches ($\mathbf{r_{11}}$, $\mathbf{r_{21}}$, $\mathbf{r_{12}}$, $\mathbf{r_{22}}$, $\mathbf{r_{13}}$, $\mathbf{r_{23}}$) are applied on it. Let us denote by $\mathbf{R}$ the matrix composed of these wrenches applied on the platform by the legs. The expression of $\mathbf{R}$ in the base frame, and expressed at point O, is

$$\mathbf{R} = \begin{bmatrix} \mathbf{r}_{11}^T \\ \mathbf{r}_{21}^T \\ \mathbf{r}_{12}^T \\ \mathbf{r}_{22}^T \\ \mathbf{r}_{13}^T \\ \mathbf{r}_{23}^T \end{bmatrix} = \begin{bmatrix} 0 & \cos\theta_1 & \sin\theta_1 & 0 & 0 & 0 \\ 0 & z_{C1} & -y_{C1} & 1 & 0 & 0 \\ \sin\theta_2 & 0 & \cos\theta_2 & 0 & 0 & 0 \\ -z_{C2} & 0 & x_{C2} & 0 & 1 & 0 \\ \cos\theta_3 & \sin\theta_3 & 0 & 0 & 0 & 0 \\ -x_{C3} & y_{C3} & 0 & 0 & 0 & 1 \end{bmatrix} \tag{5}$$

In this expression, θ_1, θ_2, and θ_3 are the angles between vectors $\mathbf{a_{11}}$, $\mathbf{a_{12}}$, and $\mathbf{a_{13}}$ and $\boldsymbol{y}$, $\boldsymbol{z}$, and $\boldsymbol{x}$ axes, respectively. Note that analyzing the condition of orthogonality on the axes of pairs ($12i$), it could be proven that angles γ_i are constrained to be equal to 0. Therefore, these terms disappear from Eq. (5).

Without loss of generality, let us consider that actuator M_3 is disconnected. Thus, the manipulator gains one passive DOF. The twist corresponding to this passive DOF is the screw $\mathbf{t_1}$, which is orthogonal to the five wrenches applied on the platform,

$$\mathbf{t_1} = [\omega_x \quad \omega_y \quad \omega_z \quad v_x \quad v_y \quad v_z]^T \tag{6}$$

where ω_x, ω_y, and ω_z correspond to the rotational velocities of the platform about $\boldsymbol{x}$, $\boldsymbol{y}$, and $\boldsymbol{z}$ axes and v_x, v_y, and v_z correspond to its translational velocities along $\boldsymbol{x}$, $\boldsymbol{y}$, and $\boldsymbol{z}$ axes. If $\mathbf{t_1}$ is a passive motion, the following relation must hold:

$$[\mathbf{r_{11}} \quad \mathbf{r_{21}} \quad \mathbf{r_{12}} \quad \mathbf{r_{22}} \quad \mathbf{r_{13}}]^T \mathbf{t_1} = \mathbf{0} \tag{7}$$

As, in Eq. (7), there are five equations for six unknowns (the components of $\mathbf{t_1}$), the system admits an infinity of solutions. Thus, without loss of generality, let us fix the value of v_z to 1. Rearranging Eq. (7) yields

$$\mathbf{R}' \begin{bmatrix} \omega_x \\ \omega_y \\ \omega_z \\ v_x \\ v_y \end{bmatrix} = \begin{bmatrix} 0 & \cos\theta_1 & \sin\theta_1 & 0 & 0 \\ 0 & z_{C1} & -y_{C1} & 1 & 0 \\ \sin\theta_2 & 0 & \cos\theta_2 & 0 & 0 \\ -z_{C2} & 0 & x_{C2} & 0 & 1 \\ \cos\theta_3 & \sin\theta_3 & 0 & 0 & 0 \end{bmatrix} \begin{bmatrix} \omega_x \\ \omega_y \\ \omega_z \\ v_x \\ v_y \end{bmatrix} = \mathbf{0} \tag{8}$$

from which, if the matrix is nonsingular, $\mathbf{t_1}$ can be found as

$$\mathbf{t_1} = [0 \quad 0 \quad 0 \quad 0 \quad 0 \quad 1]^T \tag{9}$$

We would like to mention that the case where matrix $\mathbf{R}'$ is singular will be studied later in the section about singularities. Thus, throughout the workspace of the mechanism, the permitted passive motion of the platform when actuator M_3 is disconnected is a free translation along the $\boldsymbol{z}$ axis. Thus, actuator M_3 controls the translation of the platform along the $\boldsymbol{z}$ axis. Moreover, as the axis of actuator M_3 is also directed along the $\boldsymbol{z}$ axis, it becomes obvious that due to the copying properties of the pantograph linkage, a displacement of actuator M_3 is transformed on a displacement of the platform along the same direction but amplified by the pantograph linkage.

By similar analyses, it could be proved that actuator M_1 (M_2) controls the translation of the platform along the $\boldsymbol{x}$ axis ($\boldsymbol{y}$ axis). Moreover, a displacement of actuator M_1 (M_2) is transformed on a displacement of the platform along the same direction but amplified by the pantograph linkage. Thus, the input-output relations for this manipulator are linear, and it belongs to the family of the fully decoupled 3DOF translational parallel mechanisms.

2.3 Geometric and Kinematic Models and Singularity Analysis. The origin O of the base frame is fixed such that it coincides with point P of the platform when all linear actuators

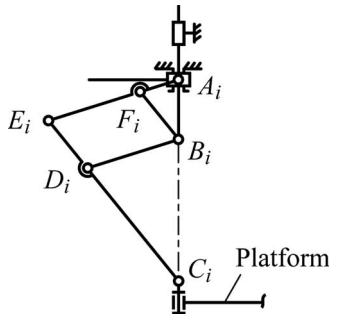

Fig. 4 Example of leg singularities

have zero length. It is also considered that an increasing actuator's length displaces the platform along the positive part of the corresponding base frame axis. Therefore, the following trivial system of decoupled linear equations governs the movement of the Pantopteron,

$$x = k(\rho_1 - x_{G1}) - a_1 \tag{10}$$

$$y = k(\rho_2 - y_{G2}) - b_2 \tag{11}$$

$$z = k(\rho_3 - z_{G3}) - c_3 \tag{12}$$

where k is the magnification factor of the pantograph linkages, x, y, and z are the coordinates of point P of the platform along $\boldsymbol{x}$, $\boldsymbol{y}$, and $\boldsymbol{z}$ axes, respectively, ρ_i is the length of actuator i, x_{G1}, y_{G2}, and z_{G3} are coordinates of points G_i of the platform along $\boldsymbol{x}$, $\boldsymbol{y}$, and $\boldsymbol{z}$ axes, respectively, and a_1, b_2, and c_3 are constant terms defining the shape of the platform (see Eq. (22)).

Since $k \neq 0$, the above system of independent equations can be inverted to give the trivial solution to the inverse kinematics of the Pantopteron. Though simple as it is, the system of independent equations (Eqs. (10)–(12)) can be rewritten in matrix form as

$$\mathbf{x} = \mathbf{J}\mathbf{q} + \mathbf{c} \tag{13}$$

where $\mathbf{x}=[x,y,z]^T$ is the vector of output Cartesian coordinates, $\mathbf{q}=[\rho_1,\rho_2,\rho_3]^T$ is the vector of input coordinates, and

$$\mathbf{J} = \begin{bmatrix} k & 0 & 0 \\ 0 & k & 0 \\ 0 & 0 & k \end{bmatrix} \tag{14a}$$

$$\mathbf{c} = -\begin{bmatrix} kx_{G1} + a_1 & ky_{G2} + b_2 & kz_{G3} + c_3 \end{bmatrix}^T \tag{14b}$$

Differentiating Eq. (13) leads to

$$\dot{\mathbf{x}} = \mathbf{J}\dot{\mathbf{q}} \tag{15}$$

Hence, $\mathbf{J}$ is the Jacobian matrix of the Pantopteron. Recall that the terms of the Jacobian matrix of the fastest Tripteron are equal to 1. Therefore, *the Pantopteron displaces* k times faster than the Tripteron (where k is obviously greater than 1). It is also clear that due to this property and to the greater number of joints in comparison with the Tripteron, the accuracy of the proposed robot will be lower. However, the purpose of this robot is not to be more accurate but to be much faster.

One type of singularities occurring in the proposed mechanism is due to the degeneracy of the kinematics of the pantograph legs. Such singularities appear when

- the parallelogram $B_iD_iE_iF_i$ degenerates into a line; near such a case of singularity, the efforts in the revolute joints located at E_i, F_i, D_i, and B_i grow considerably, so it has to be avoided by limiting the angle between links (A_iE_i) and (E_iC_i).
- points A_i, B_i, and C_i are aligned along the same axis (Fig. 4); in such a case, given one position of the platform, there is infinity of orientations for the pantograph linkage. Moreover, if during a displacement of the mechanism, a leg comes close from this singularity, the angular velocity of the pantograph linkage around the axis defined by segment (G_iB_i) becomes very high. Therefore, the neighborhood of such configurations should be avoided by limiting the displacement of pair $(9i)$.

These two kinds of singularity define the boundaries of the workspace. They are similar to the singular configurations that we can meet in the Tripteron.

A second case of singularities appears if the system of wrenches applied on the platform degenerates, i.e., if the matrix $\mathbf{R}$ of Eq. (5) becomes singular. Such a singularity is called a constraint singularity [18]. This happens if

$$\det(\mathbf{R}) = \cos\theta_1 \cos\theta_2 \cos\theta_3 + \sin\theta_1 \sin\theta_2 \sin\theta_3 = 0 \tag{16}$$

In such a case, the three moments applied on the platform are linearly dependent; i.e., their axes are parallel or coplanar. Thus, the platform becomes unconstrained, and it gains one supplementary DOF.

Let us observe the example presented in Fig. 5. Axis $\mathbf{a_{11}}$ is parallel to the $\boldsymbol{y}$ axis, and axes $\mathbf{a_{12}}$ and $\mathbf{a_{13}}$ are parallel to the $\boldsymbol{x}$

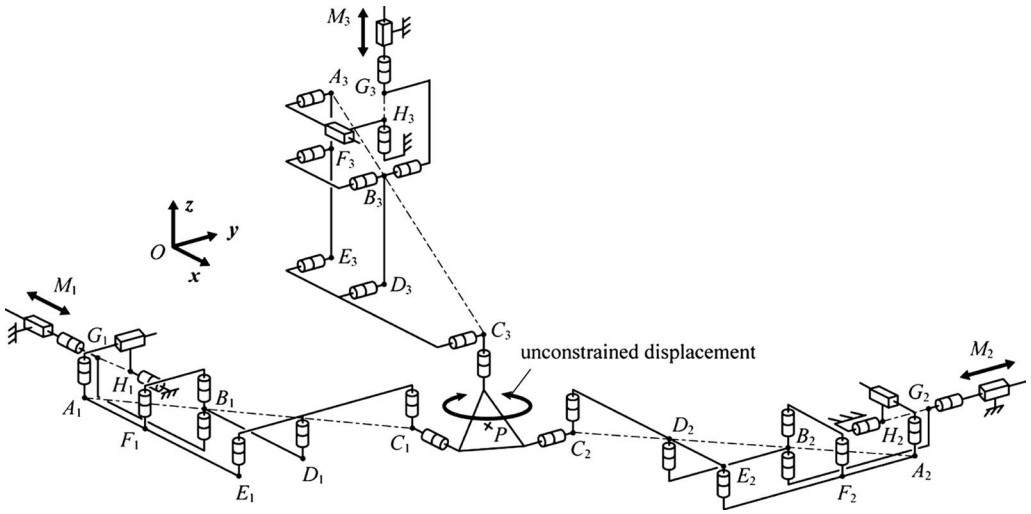

Fig. 5 Example of a constraint singularity

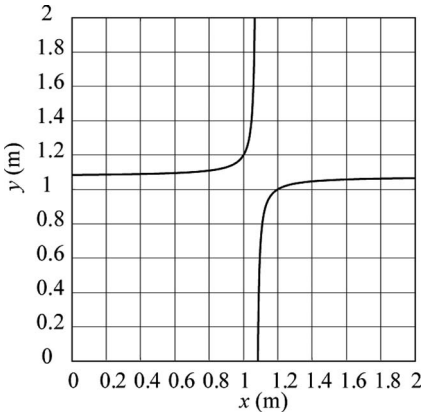

Fig. 6 Example of constraint singularity loci

axis. Thus, the gained DOF of the platform is a rotation about an axis parallel to the z axis.

Expressing Eq. (16) in the Cartesian space, it becomes

$$\det(\mathbf{R}) = \frac{(y_{C1}-y_{G1})(z_{C2}-z_{G2})(x_{C3}-x_{G3})}{\Gamma_1\Gamma_2\Gamma_3} + \frac{(z_{C1}-z_{G1})(x_{C2}-x_{G2})(y_{C3}-y_{G3})}{\Gamma_1\Gamma_2\Gamma_3} = 0 \quad (17)$$

where

$$\Gamma_1 = \sqrt{(y_{C1}-y_{G1})^2 + (z_{C1}-z_{G1})^2} \quad (18)$$

$$\Gamma_2 = \sqrt{(z_{C2}-z_{G2})^2 + (x_{C2}-x_{G2})^2} \quad (19)$$

$$\Gamma_3 = \sqrt{(x_{C3}-x_{G3})^2 + (y_{C3}-y_{G3})^2} \quad (20)$$

In these expressions, x_{Ci}, y_{Ci}, and z_{Ci} and x_{Gi}, y_{Gi}, and z_{Gi} correspond to the coordinates of points C_i and G_i about $\boldsymbol{x}$, $\boldsymbol{y}$, and $\boldsymbol{z}$ axes, respectively. Disregarding the case where Γ_i tends to infinity, singularities appear when

$$(y_{C1}-y_{G1})(z_{C2}-z_{G2})(x_{C3}-x_{G3}) + (z_{C1}-z_{G1})(x_{C2}-x_{G2})(y_{C3}-y_{G3}) = 0 \quad (21)$$

Taking into account that the terms x_{Gi}, y_{Gi}, and z_{Gi} appearing in Eq. (21) are constant and that

$$\mathbf{OC}_i = [x,y,z]^T + [a_i,b_i,c_i]^T \quad (22)$$

where a_i, b_i, and c_i are constant terms, Eq. (21) can be rewritten under the form

$$p_1xyz + p_2xy + p_3xz + p_4yz + p_5x + p_6y + p_7z + p_8 = 0 \quad (23)$$

where coefficient p_i are constant terms depending on the position of points G_i and on the shape of the platform. Fixing the altitude z of the platform, Eq. (23) is the expression of a hyperbola, whose coefficients depend on the altitude of the platform and on the geometric parameters of the mechanism.

Figure 6 presents an example of the constraint singularities in the workspace of a Pantopteron with the following characteristics:

- z=0.5 m
- $\mathbf{OC_1}$=[−0.2 m,−0.2 m,0 m]^T, $\mathbf{OC_2}$=[0 m,−0.2 m,0.2 m]^T, and $\mathbf{OC_3}$=[−0.2 m,0 m,0.2 m]^T
- $y_{G1}=z_{G1}=x_{G2}=z_{G2}=x_{G3}=y_{G3}$=1 m
- the parameters of the pantograph linkages are irrelevant but allow a workspace comprised of the interval $x,y \in$[0 m,2 m]

We would like to mention that our mechanism, contrary to the Tripteron, has constraint singularities. This is due to the fact that each leg of the Tripteron is attached to the platform by a revolute joint, instead of a Cardan joint, which overconstrains the displacement of the platform and allows avoiding such singular configurations. However, it will be shown in the following section that even if the Pantopteron has singularities, they can easily be removed from its workspace.

3 Design Considerations

In this part, we will perform the analysis of the workspace of the mechanism, taking into account the geometric limitations and singular configurations, and discuss about some other possible architectures based on this mechanism.

3.1 Geometric Workspace Analysis. Many parameters influence the size of the workspace of the Pantopteron. As the main parameters, we can mention

- the lengths of the links of the pantograph
- the locations of the axes of the base-mounted revolute joints
- the shape of the platform
- the maximal stroke of the actuators and of the passive linear guide
- the interference between the links
- the singular configurations

Using the geometric approach, we will compute the workspace of the Pantopteron. As the Pantopteron is a translational parallel mechanism, its workspace can be found as the intersection of three so-called vertex spaces.

Analyzing the vertex space of leg i, it only depends on

- the lengths of the links of the pantograph
- the maximal and minimal strokes of the actuators and of the passive linear guide
- the interferences between the links
- the singular configurations

In the first step, let us concentrate on the boundaries of the workspace due to the interference of the links and of the singular configurations. As mentioned previously, for a leg, there are two types of singularities:

(a) When the parallelogram $B_iD_iE_iF_i$ degenerates into a line; such a singularity can be avoided by limiting the angle α_i between the links (A_iE_i) and (E_iC_i) of the parallelogram, which, at the same time, allows limiting some inferences between the links. The maximal and minimal angles will be denoted as $(\alpha_i)_{\max}$ and $(\alpha_i)_{\min}$, respectively.

(b) When points A_i, B_i, and C_i are aligned along the same axis; such a case can easily be avoided by limiting the stroke of the passive prismatic pair (9i). This minimal stroke will be denoted as $(s_i)_{\min}$.

To avoid interference between the links and the base, a maximal stroke of the actuator has to be fixed at $(\rho_i)_{\max}$.

Each leg is mounted in rotation around one axis parallel to $\mathbf{a}_{3i}$. Thus, the problem of finding the vertex space can be limited to a planar analysis of the minimal and maximal displacements of point C_i, the entire vertex space being found by the symmetry of revolution of these displacements.

Considering case (a), we have to find the boundaries of the leg when angle α_i is fixed. Fixing angle α_i is equivalent to fixing the lengths of segments (A_iB_i) and (A_iC_i). These lengths are equal to

$$l_{AiCi} = l_{EiCi}^2 + l_{AiEi}^2 - 2l_{AiEi}l_{EiCi}\cos\alpha_i \quad (24)$$

$$l_{AiBi} = l_{AiCi}/k \quad (25)$$

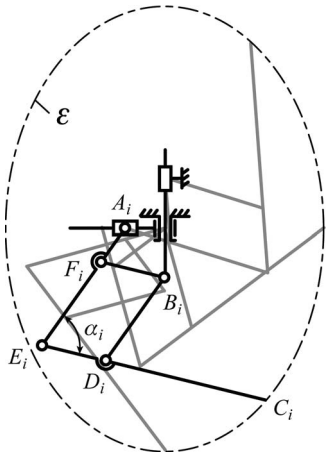

Fig. 7 Displacement of C_i when α_i is fixed

Displacing the prismatic guides, segments (A_iB_i) and (B_iC_i) describe Cardanic motions [19,20]. As a result, for a given angle α_i, the displacement locus of point C_i is an ellipse $\mathcal{E}$ (Fig. 7). Thus, considering the extremes $(\alpha_i)_{\max}$ and $(\alpha_i)_{\min}$ of angle α_i, the boundaries of the workspace are given by the ellipses $\mathcal{E}_{\min}$ and $\mathcal{E}_{\max}$ (Fig. 8(*a*)).

Cases (b) and (c) are much simpler to analyze. The displacement of point C_i when the passive guide $(9i)$ is at its minimal stroke $(s_i)_{\min}$ is a vertical line $\mathcal{L}_1$ located at $(k-1)$ times the distance $(s_i)_{\min}$ from the vertical axis (G_iB_i) (Fig. 8(*a*)). The displacement of point C_i when actuator M_i is at its maximal stroke $(\rho_i)_{\max}$ is a horizontal line $\mathcal{L}_2$ located at k times the distance between the maximal position of point B_i and the position of point A_i along axis $\mathbf{a}_{3i}$ from the axis of the horizontal passive guide $(9i)$ (Fig. 8(*a*)).

The entire vertex space is represented in Fig. 8(*b*). On all of these figures, two boundaries due to two constraints, which are the maximal strokes of the actuated and passive linear joints, are not represented. These boundaries are vertical and horizontal straight lines. However, in the first step, it is preferable to have the largest

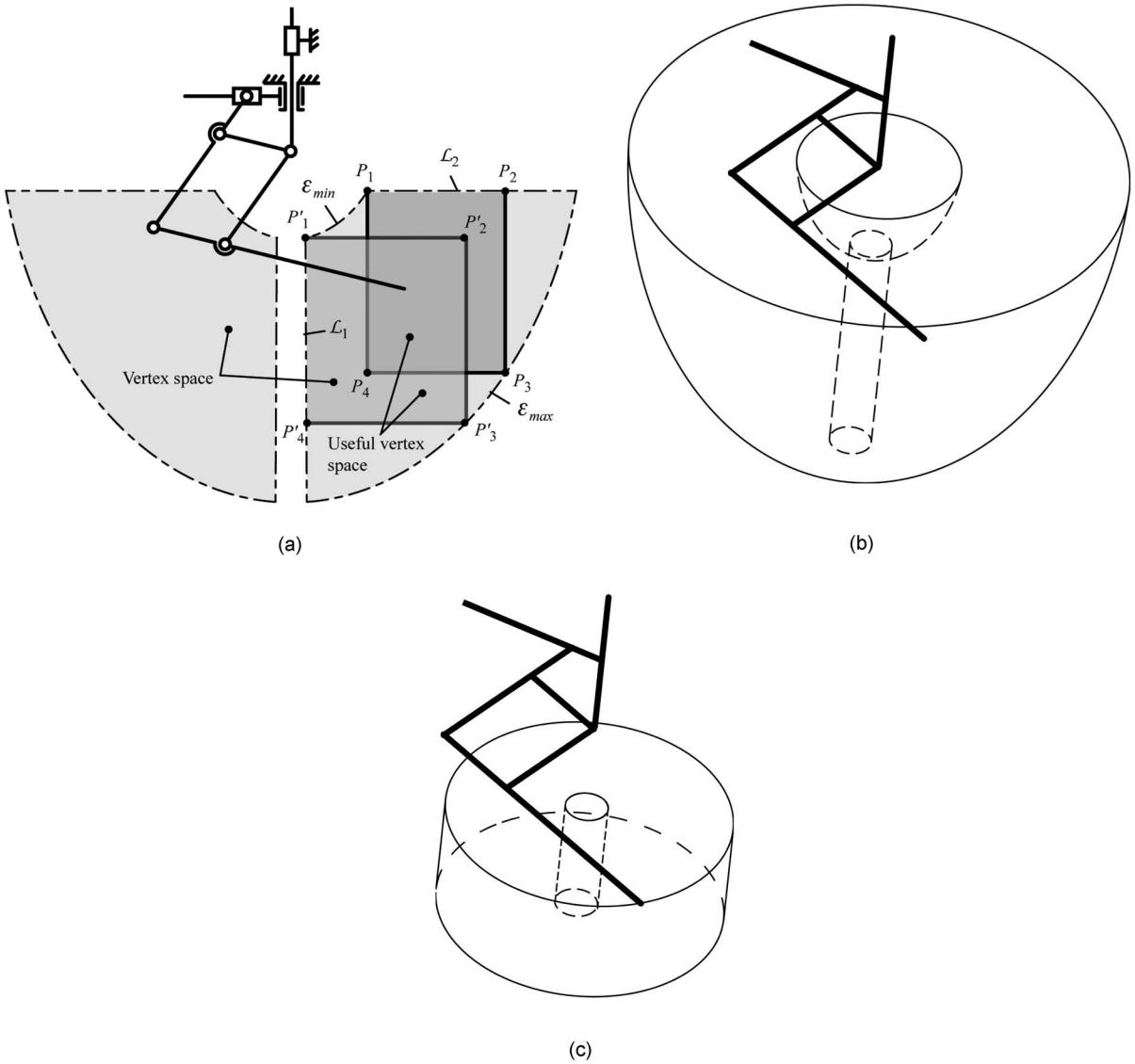

Fig. 8 Schematics of the vertex space of a leg from the Pantopteron: (*a*) planar projection of the vertex space, (*b*) the 3D vertex space of the leg, and (*c*) the 3D useful vertex space of the leg

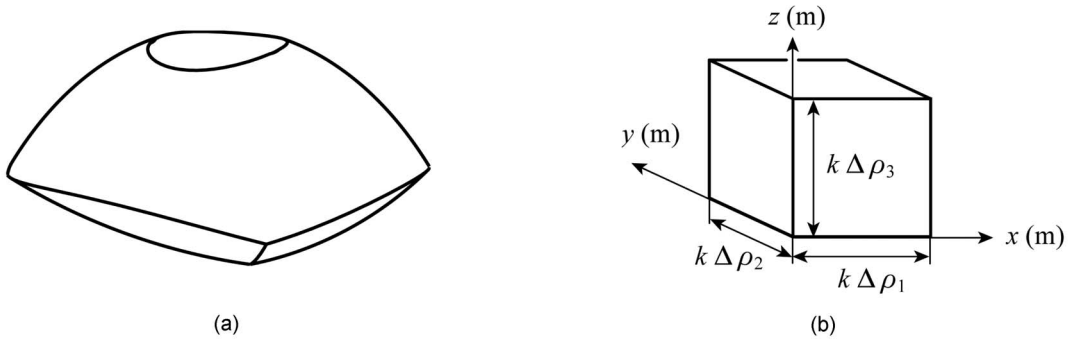

Fig. 9 Workspace of the Pantopteron: (*a*) with relatively short legs and (*b*) with relatively long legs

vertex space for the legs and, thus, to remove these two boundaries out of our workspace by a proper design of the stroke of the linear guides.

As researchers, the first thing on our mind was to implement in MATLAB our geometric method in order to be able to optimize the workspace of the Pantopteron by minimizing the lengths of the pantograph's links in each leg. This could be done more promptly in a commercial computer aided design (CAD) system, such as CATIA [21]. Figure 9(*a*) shows an example of the workspace of a Pantopteron with relatively short legs. We can obtain the best ratio between the lengths of the links and the volume of the workspace. A relatively large increase in the link lengths will result in only a negligible gain in the workspace volume.

Obviously, it would be a mistake to design a Cartesian parallel mechanism with a complex workspace. Thus, our decision is to keep the links as long as it takes, so that the workspace of the mechanism becomes a simple geometric form, namely, a rectangular parallelepiped. In other words, the workspace of a Pantopteron with sufficiently long legs has to become a box whose sides are of length $k\Delta\rho_i$ ($\Delta\rho_i$ being the stroke of actuator M_i), as shown in Fig. 9(*b*).

In order to obtain such a simple volume, when the three vertex spaces are intersected, it is the planar caps that limit the workspace and not the other surfaces. Of course, we still try to minimize the length of the links by carefully locating the prismatic actuators on the base and properly choosing the dimensions of the mobile platform and of the stroke of the actuators. Furthermore, if the workspace of the mechanism has to be a parallelepiped, the shape of the vertex space does not have to be so complicated and can be reduced to a hollow cylinder (Fig. 8(*c*)). This can be accomplished by properly constraining the maximal stroke of the active and passive linear guides in order to obtain, in the planar projection of the workspace, a rectangle denoted as the useful vertex space (two possible examples of the useful vertex space are presented in Fig. 8(*a*)).

The size of the workspace of the Pantopteron is the other main advantage of the proposed robot. Indeed, the maximal volume of the workspace of the Tripteron is $V=\Delta\rho_1\Delta\rho_2\Delta\rho_3$, while that of the Pantopteron is $V=k^3\Delta\rho_1\Delta\rho_2\Delta\rho_3$; i.e., for the same set of given actuators, the workspace of the Pantopteron is k^3 times bigger than that of the Tripteron.

Moreover, it is well known that the actuators represent at least 80% of the global cost of a robot. For creating a fast mechanism with actuated prismatic pairs, it is now preferable to use electric linear actuators that reach higher velocities. However, the main drawback of such actuators is their price, which is proportional to the length of their stroke. For a given maximal workspace, the stroke of the actuators of the Tripteron is k times greater than that of the motors of the Pantopteron. Therefore, even if the Pantopteron is more complicated to design than a Tripteron, its manufacturing cost would likely be lower.

3.2 Singularity-Free Workspace. It is impossible to speak about the workspace of a parallel mechanism without dealing with singularities. As seen previously from Eq. (23), the singular configurations depend on the position of the mobile platform, on the locations of the axes of the base-mounted revolute joints, and on the shape of the platform. Thus, analyzing Eq. (23), there are 12 design parameters, which are y_{G1}, z_{G1}, x_{G2}, z_{G2}, x_{G3}, y_{G3}, b_1, c_1, a_2, c_2, a_3, and b_3 (we do not consider the lengths of the links of the pantograph linkages as they do not influence these singular configurations). So, there is too much parameter in order to perform a complete analysis of the singular configurations. However, it is possible to restrict our analysis to some particular designs, which will decrease the number of parameters.

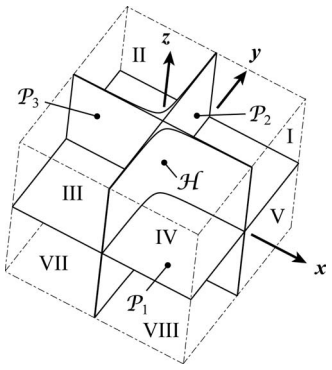

Fig. 10 Singularity-free workspaces

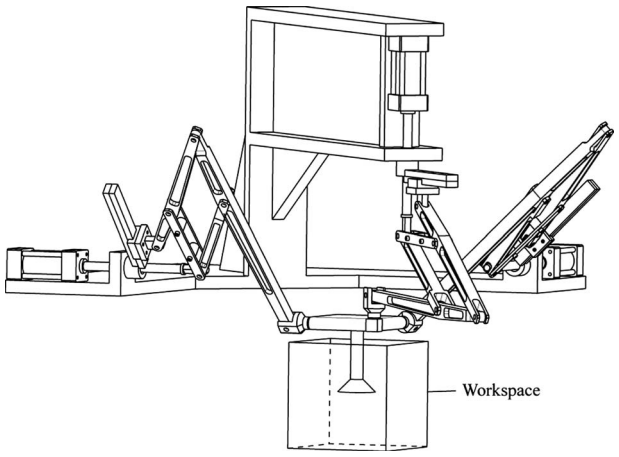

Fig. 11 CAD view of the prototype of Pantopteron

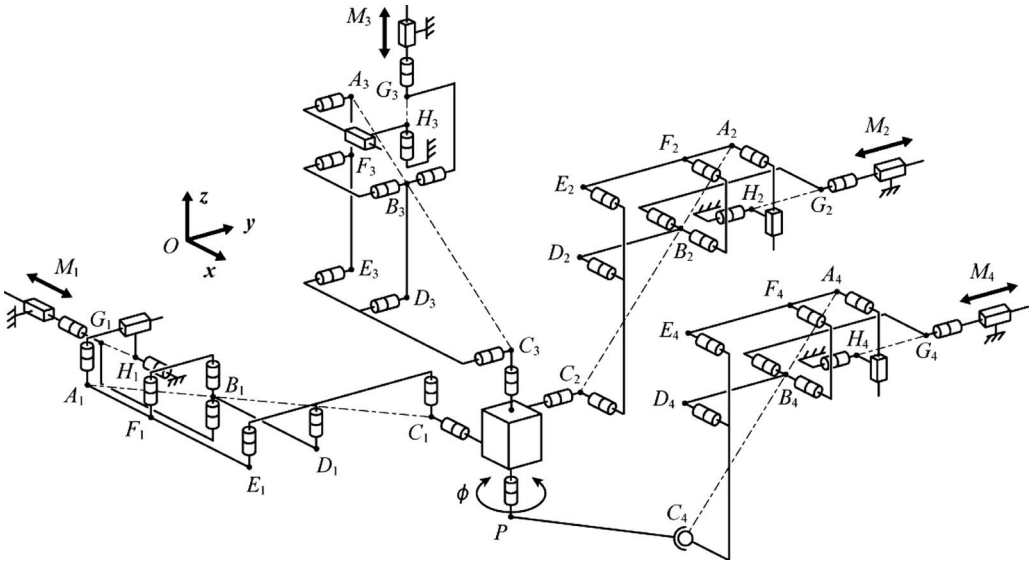

Fig. 12 Pantopteron with 4DOF

Thus, we will consider in this part a mechanism that will have a platform with two axes concurrent (for example, for pairs (12,1) and (12,3)) and a base of which two axes of actuators are also concurrent (for example, those of actuators M_1 and M_2). Therefore, considering that the intersection point of the axes of actuators M_1 and M_2 is the origin of the base frame and that point P is at the intersection of the two axes of the platform, only x_{G3}, y_{G3}, a_3, and b_3 remain as variables, the other ten parameters being equal to zero.

In such a case, Eq. (23) becomes

$$z(2xy + y(a_3 - x_{G3}) + x(b_3 - y_{G3})) = 0 \tag{26}$$

Thus, singular configurations will appear if the platform of the mechanism is located in plane $\mathcal{P}_1$ ($z=0$) or if it is located on a hyperbola $\mathcal{H}$ whose expression is

$$2xy + y(a_3 - x_{G3}) + x(b_3 - y_{G3}) = 0 \tag{27}$$

Please note that this expression does not depend on the altitude z of the platform. It is well known that such a hyperbola has two asymptotes,

$$y = (y_{G3} - b_3)/2 \tag{28}$$

$$x = (x_{G3} - a_3)/2 \tag{29}$$

which, in 3D, represent two planes $\mathcal{P}_2$ and $\mathcal{P}_3$. Thus, the Cartesian space may be separated into eight regions (Fig. 10). In regions I, III, V, and VII, there are no singularities, and it will be quite easy to develop a manipulator of which the workspace is located in these regions, taking into account the previous geometric approach. In regions II, IV, VI, and VIII, even if there are singular configurations, they are quite close from planes $\mathcal{P}_2$ and $\mathcal{P}_3$, and thus, it is also quite easy to inscribe a cube representing the workspace of the mechanism in these regions.

Please note that in the special cases where all parameters are equal to zero, or $a_3=x_{G3}$ and $b_3=y_{G3}$, Eq. (26) becomes

$$2xyz = 0 \tag{30}$$

Thus, the hyperbolas degenerate into two straight lines of equations $x=0$ and $y=0$. Therefore, the eight regions delimited by planes $\mathcal{P}_i$ have no singularities.

A possible version of a prototype of a Pantopteron is represented in Fig. 11. Its geometric parameters are

- $l_{AiEi}=0.2$ m, $l_{EiCi}=0.3$ m, and $k=3$
- $y_{G1}=z_{G1}=x_{G2}=z_{G2}=x_{G3}=y_{G3}=0$ m and $b_1=c_1=a_2=c_2=a_3=b_3=0$ m
- actuator strokes=0.06 m$((z_i)_{\min}=-0.22$ m$,(z_i)_{\max}=-0.16$ m)
- passive linear guide strokes=0.14 m$((s_i)_{\min}=0.01$ m$,(s_i)_{\max}=0.15$ m)
- $(\alpha_i)_{\min}=25$ deg and $(\alpha_i)_{\max}=155$ deg

Its design is achieved such as its workspace is a cube whose side is equal to 0.18 m.

3.3 Other Possible Architectures. Finally, we would like to mention that the design of the Pantopteron presented here is not the only solution for creating such a mechanism. First, as the leg is made up of a pantograph linkage, several designs are possible, which are presented in Ref. [22]. However, we think that the architecture we proposed is the most practical one. Moreover, note that the planar *RP* chain composed of the revolute joint (10*i*) and the prismatic joint (9*i*) could be removed and replaced by any kinematic chain able to perform a planar displacement, as planar *RRR*, *RPR*, *PPR*, or *PRR* chains. Moreover, using such chains, points H_i and G_i need not be aligned.

Note also that other architectures with various DOFs are possible by modifying our Pantopteron, such as the mechanism with four decoupled DOFs represented it Fig. 12.

4 Conclusions

In this paper, a novel 3DOF fully decoupled isotropic translational parallel mechanism, named the Pantopteron, was presented. This mechanism is very similar to the Tripteron Cartesian parallel mechanism, but due to its architecture, which is made of three pantograph linkages, an amplification of the movements between the actuators and the platform displacements is achieved. Therefore, the Pantopteron displaces k times faster than the Tripteron (k being the magnification factor of the pantograph linkages). Moreover, for a given set of actuators, its workspace is k^3 times bigger than that of the Tripteron. Due to this property, if the size of the workspace is given, the stroke of the actuators of the Pantopteron is k times smaller than that of the Tripteron, which allows reducing the manufacturing cost. This novel mechanism is foreseen to be used in applications where the velocities and accelerations have to be high, such as in pick-and-place.

References

[1] Gosselin, C. M., and Kong, X., 2004, "Cartesian Parallel Manipulators," U.S. Patent No. 6,729,202.

[2] Carricato, M., and Parenti-Castelli, V., 2002, "Singularity-Free Fully-Isotropic Translational Parallel Manipulators," Int. J. Robot. Res., **21**(2), pp. 161–174.

[3] Kong, X., and Gosselin, C. M., 2002, "Type Synthesis of Linear Translational Parallel Manipulators," *Advances in Robot Kinematics: Theory and Applications*, J. Lenarcic and F. Thomas, eds. (Kluwer Academic, Dordrecht), pp. 453–462.

[4] Kong, X., and Gosselin, C. M., 2002, "A Class of 3-DOF Translational Parallel Manipulators With Linear Input-Output Equations," Proceedings of the Workshop on Fundamental Issues and Future Research Directions for Parallel Mechanisms and Manipulators, Quebec City, Quebec, Canada, Oct. 3–4, pp. 25–32.

[5] Kim, H. S., and Tsai, L. W., 2002, "Evaluation of a Cartesian Parallel Manipulator," *Advances in Robot Kinematics: Theory and Applications*, J. Lenarcic and F. Thomas, eds. (Kluwer Academic, Dordrecht), pp. 21–28.

[6] Hervé, J. M., and Sparacino, F., 1991, "Structural Synthesis of Parallel Robots Generating Spatial Translation," *Proceedings of the 5th IEEE International Conference on Advanced Robotics*, Pisa, Italy, pp. 808–813.

[7] Gogu, G., 2008, *Structural Synthesis of Parallel Robots, Part 1—Methodology* (Springer, The Netherlands).

[8] Gogu, G., 2004, "Structural Synthesis of Fully-Isotropic Translational Parallel Robots Via Theory of Linear Transformations," Eur. J. Mech. A/Solids, **23**(6), pp. 1021–1039.

[9] Carricato, M., and Parenti-Castelli, V., 2004, "A Novel Fully Decoupled 2-DOF Parallel Wrist," Int. J. Robot. Res., **23**(6), pp. 661–667.

[10] Callegari, M., Palpacelli, M., and Scarponi, M., 2005, "Kinematics of the 3-CPU Parallel Manipulator Assembled for Motions of Pure Translation," *Proceedings of the 2005 IEEE International Conference on Robotics and Automation (ICRA)*, Barcelona, Spain.

[11] Ruggiu, M., 2008, "Kinematic Analysis of the CUR Translational Manipulator," Mech. Mach. Theory, **43**(9), pp. 1087–1098.

[12] Lee, C.-C., and Hervé, J. M., 2007, "Cartesian Parallel Manipulators With Pseudoplanar Limbs," ASME J. Mech. Des., **129**, pp. 1256–1264.

[13] Li, W., Zhang, J., and Gao, F., 2006, "P-CUBE, A Decoupled Parallel Robot Only With Prismatic Pairs," Proceedings of the Second IEEE/ASME International Conference on Mechatronic and Embedded Systems and Applications, Beijing, China.

[14] Pierrot, F., Nabat, V., Company, O., Krut, S., and Poignet, P., 2008, "Optimal Design of a 4-dof Parallel Manipulator: From Academia to Industry," IEEE Trans. Rob. Autom., in press.

[15] Bonev, I. A., 2001, "Delta Robot—The Story of Success," online article available at www.parallemic.org/Reviews/Review002.html.

[16] Briot, S., Arakelian, V., and Guégan, S., 2009, "PAMINSA: A New Family of Decoupled Parallel Manipulators," Mech. Mach. Theory, **44**(2), pp. 425–444.

[17] Briot, S., Arakelian, V., and Guégan, S., 2008, "Design and Prototyping of a Partially Decoupled 4-DOF 3T1R Parallel Manipulator With High-Load Carrying Capacity," ASME J. Mech. Des., **130**(12), p. 122303.

[18] Zlatanov, D., Bonev, I. A., and Gosselin, C. M., 2002, "Constraint Singularities of Parallel Mechanisms," IEEE International Conference on Robotics and Automation (ICRA 2002), Washington, DC, May 11–15.

[19] Sekulie, A., 1998, "Method of Synthesis of Cardanic Motion," Facta Universitatis, Series Mechanical Engineering, University of NIS, **1**(5), pp. 565–572.

[20] Tischler, C. R., Hunt, K. H., and Samuel, A. E., 1998, "A Spatial Extension of Cardanic Movement: Its Geometry and Some Derived Mechanisms," Mech. Mach. Theory, **33**(8), pp. 1249–1276.

[21] Bonev, I. A., and Ryu, J., 2001, "A Geometrical Method for Computing the Constant-Orientation Workspace of 6-PRRS Parallel Manipulators," Mech. Mach. Theory, **36**(1), pp. 1–13.

[22] Lu, D.-M., and Hwang, W.-M., 1996, "Synthesis of Planar Five-Bar Pantograph Configurations by a Geometric Method," Mech. Mach. Theory, **31**(1), pp. 11–21.